J Therm Anal Calorim (2017) 130:2093–2103
DOI 10.1007/s10973-017-6714-5

Real-time thermo-optical analysis of polymer samples by quantitative polarized optical microscopy

Luciana Assumpção Bicalho[1] · Jorge Manuel Jardim da Silva[1] · José António Covas[2] · Sebastião Vicente Canevarolo[3]

Received: 22 December 2016 / Accepted: 13 September 2017 / Published online: 25 September 2017

Abstract An experimental setup using a polarized optical microscope fitted with a detection module capable of measuring the cross-polarized transmitted light intensity and the transmitted light intensity of the polymer sample being analyzed, together with an accompanying calculation procedure, is proposed in order to characterize in real-time thermal transitions and degree of crystallinity, as well as birefringence (which is a measure of orientation) and turbidity. The experimental assessment of the technique was carried out studying commercial poly(ethylene terephthalate) multifilaments with different crystallinity and stretching levels and by direct comparison with the features of conventional DSC curves obtained under similar experimental conditions. While an excellent correlation was found between the type and temperature ranges of thermal events as detected by thermal and optical techniques, the measured birefringence was shown to be sensitive to distinct filament stretching levels, but unaffected by geometrical factors. Contrarily, turbidity is influenced by the latter.

✉ Sebastião Vicente Canevarolo
caneva@ufscar.br

[1] Programa de Pós-Graduação em Ciência e Engenharia de Materiais – PPG-CEM, Universidade Federal de São Carlos – UFSCar, Rod. Washington Luís, km 235, São Carlos 13565-905, Brazil

[2] Departamento de Engenharia de Polímeros, IPC/I3N, Universidade do Minho, Guimarães, Campus de Azurém, 4800-058 Guimarães, Portugal

[3] Departamento de Engenharia de Materiais - DEMa, Universidade Federal de São Carlos - UFSCar, Rod. Washington Luís, km 235, São Carlos 13565-905, Brazil

Keywords Birefringence · Optical path difference · Polarized light microscopy · Poly(ethylene terephthalate) · Thermo-optical behavior

Introduction

The performance of thermoplastic parts under service is strongly determined by the intrinsic properties of the polymer(s) and by the morphology created during processing, namely the degree of crystallinity and molecular orientation. These characteristics can be accessed by various experimental techniques [1–3], but only a few are feasible for routine utilization for quality control purposes within an industrial production environment. The degree of crystallinity can be readily estimated by differential scanning calorimetry (DSC), subjecting the sample to a specific temperature program after adequate calibration and upon knowledge of the enthalpy of the 100% crystalline material [4]. The determination of optical properties can also provide related information. Since turbidity depends on the size and extent of the existing structural order (or of suspended particles) [5], the measurement of its intensity should provide an estimate of the degree of crystallinity, with the advantage of avoiding the need to subject the material to a thermal cycle as required by DSC. The intensity of molecular orientation can be appraised in terms of birefringence, which can be determined by polarized optical microscopy (POM). Magill [6, 7] and Spruiell and co-workers [8–10] followed the crystallization kinetics of various polymers. Coupling a camera and a detection device to an optical microscope, it became possible to quantify in real-time changes in polarized transmitted light intensity caused by variations in the material birefringence.

DSC and POM are widespread laboratory characterization techniques, but they entail time-consuming and relatively complex operation, as well as careful sample preparation. Therefore, they are not effective for practical process quality control, as there will be a significant delay between sample collection from the production line and the result of a measurement. Thus, it would be interesting to develop a characterization technique capable of providing real-time quantitative data on both crystallinity and orientation levels. This work proposes a quantitative POM (q-POM) technique to obtain in real-time information on crystallinity and orientation levels, taking advantage of the expected parallelism between changes in cross-polarized transmitted light intensity and thermophysical phenomena for a given partially crystalline and/or oriented polymer sample subjected to a specific thermal cycle. The setup and corresponding methodology are presented and validated using, as a case study, commercial PET filaments extruded under distinct processing conditions.

The work reported here is a first step toward the development and use of inexpensive optical devices in the production floor to support quality control during polymer processing. Indeed, the authors have been dedicated to the development and application of in-line rheo-optical techniques for material/process characterization, process optimization and quality control. Optical, spectroscopic and rheometric techniques (e.g., in-line measurements at the die during extrusion and compounding) were presented [11–13].

The application of q-POM to commercial PET filaments is discussed here, given the practical importance of accurately measuring T_g for optimal fiber of fabric dyeing performance, as discussed extensively by De Clerck et al. [14].

Experimental

Materials

Commercial poly(ethylene terephthalate) (PET) multifilaments produced by two companies—hence likely to exhibit distinct crystallinity and molecular orientation—were used (specific polymer grades and processing conditions remained undisclosed). *PET/micro* was generously donated by UNIFI Textiles (Brazil). It consists of 100 microfibers and contains 0.03 w/w% of titanium dioxide. *PET/HS* and *PET/LS* were kindly offered by ECOBRAS (Brazil). They were manufactured using the same polymer, but the first was subjected to higher stretching levels. Table 1 presents the physical characteristics of the three commercial products. The number and average diameter of individual fibers/monofilaments were determined with a Leica LEITZ DMRXP POM coupled to a Carl Zeiss Microimaging GmbH/AxioCam ERc 5s digital camera and the AxioCam ERc 5s Rev.1-2 software. The optical path difference (OPD) at room temperature was measured using a Berek's compensator (this accesses the wavelength retardation of a birefringent material), with the samples being manually aligned at 45° in relation to the crossed polarizers [15, 16]. The birefringence (Δn) was calculated knowing the filament diameter (D) and the optical path difference (using the expression $\mathrm{OPD} = D \times \Delta n$). Nonetheless, since the Berek's compensator can only measure OPD values up to 2750 nm (i.e., $\mathrm{OPD}_{max} = 5\lambda$), the exact number for *PET/HS* could not be retrieved (but will be estimated using the procedure proposed here). The degree of crystallinity was determined by DSC as explained latter.

Table 1 Physical characteristics of the PET multifilaments used in this study

Type of PET multifilament	No. of individual fibers/filaments	Filament diameter/μm
PET/micro	100	9 ± 1
PET/LS	25	54 ± 2
PET/HS	50	23 ± 2

Although *PET/LS* and *PET/HS* were produced under different processing conditions (for instance, the number of individual filaments is distinct), thus hindering a direct comparison, the smaller diameter *PET/HS* must have resulted from higher stretching and translated into much higher birefringence and higher degree of crystallinity. Comparisons with *PET/micro* are riskier, as different polymer grades were most likely utilized and titanium dioxide has a nucleating effect. Since birefringence and degree of crystallinity of *PET/micro* are relatively large and the individual filaments are much smaller, the material was possibly subjected to significant stretching during processing.

For a specific set of tests, the multifilaments were embedded in a linear low-density polyethylene matrix [DOW LLDPE 8335, with a density of 0.926 and a melt flow index of 35 g/10 min (2.16 kg/190 °C)], due to its low birefringence (thus, not masking that of the filaments) and low melting temperature. For this purpose, LLDPE flat films with an average thickness of 10 μm were extruded beforehand (using an AXPlaticos ChillRoll Ax-16/lab16 mini-extrusion line for cast film). A fixed amount of PET filaments was deposited on a LLDPE film sample with predefined dimensions and covered by another LLDPE film sample. The assemblage was subjected to compression molding (using a Luxor LPB-35-15 press) at 130 °C, under a pressure of 11 MPa during 5 min, yielding a composite

film with a thickness of approximately 30 μm and 20% w/w fiber concentration. Films containing multifilaments aligned in a single direction or randomly oriented were prepared in this way. Ensuring that the filaments remained aligned and straight during compression molding was not easy, a special filament holder having been designed and used for that purpose.

Quantitative polarized optical microscopy, q-POM

The experimental setup is illustrated in Fig. 1. It consists of a polarized light optical microscope (Leica LEITZ DMRXP) (1) coupled to a hot-stage and shearing system (CSS 450 Cambridge Shearing System) (2) that subjects the test specimens to preset thermal cycles. A homemade detection module (3) is positioned on the slot of the microscope, differently than that suggested by Spruiell [9, 10] who placed the photodetectors in the ocular lens, thereby avoiding the interference of the residual birefringence of the beam splitter. This module contains two photocells (light dependent resistors, LDRs) and an analyzer filter located just before one of the LDRs. A signal-handling box (4) converts the LDR signals (i.e., the synchronous light intensities with/without analyzer) into voltages, which are then converted into digital signals by means of an analogic–digital interface (USB data acquisition NI-DAQ 6812) (5). In turn, these signals are sent to a personal computer (6) running software developed in the LabView 8.6 NI platform (from National Instruments) that is able to perform data collection, real-time calculations, screen presentation and data saving. Additionally, this software controls the parameters of the CSS 450 control module (7) of the hot stage (2) and depicts the images captured by the CCD camera (8) attached to the microscope (1).

The white light beam emitted by the microscope lamp (9) is polarized upon passing through the polarizer filter (10), before reaching the sample placed in the hot stage (2). After interfering with the sample, this polarized light reaches the pair of photocells set in the detection module (3). The first photocell measures the reduction in the transmitted light intensity due to light scattering in the sample, i.e., its turbidity. The second, covered by an analyzer filter, measures the light retardation given as cross-polarized transmitted light intensity, which is directly related to the OPD in the sample and so to its birefringence. Simultaneously, the digital camera (8) records images of the sample. When a partially crystalline/oriented sample placed in the hot stage is subjected to heating at a fixed rate, the cross-polarized transmitted light intensity will typically exhibit several maxima and minima, thus indicating that the OPD goes through several optical orders. These variations should occur within the temperature ranges associated with morphological transitions which, if either exothermic or endothermic, can be detected by DSC scans at the same heating rate. Details on the setup and related experimental technique can be found elsewhere [17, 18].

Retrieving the cross-polarized transmitted light intensity curve does not suffice to obtain directly the total OPD values, since the optical order in which the samples lies is unknown. Using illumination with white light, passing

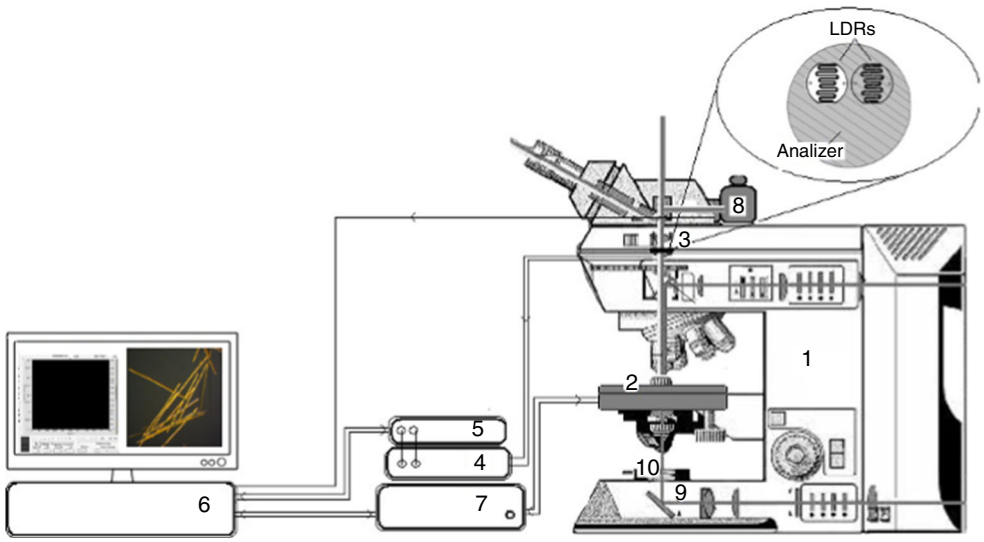

Fig. 1 Experimental setup for quantitative polarized optical microscopy (q-POM). (1) Optical microscope; (2) CSS 450 hot-stage containing sample; (3) detection module (the detailed view shows the two LDRs, one with another without analyzer); (4) signal-handling box; (5) analogical/digital interface; (6) personal computer with control and data handling software; (7) CSS 450 control module; (8) digital CCD camera; (9) lamp; (10) polarizer

from one optical order to the following one is associated with the magenta interference color, as shown by the Michel–Levy's chart. On the other hand, using monochromatic light with a fixed known wavelength, the light intensity will go through a sequence of alternating maxima and minima, forming interference fringes. For instance, if the wavelength of the monochromatic light is fixed at $\lambda = 550$ nm (i.e., green light), the minima and maxima of light intensity should occur for OPD values that are multiple of $\lambda/2 = 275$ nm. Thus, monitoring simultaneously the cross-polarized transmitted light intensity and the evolution with temperature of the filaments color (through the CCD camera), it is possible to accurately track the progress of OPD (see Fig. 4, to be discussed in "DSC versus q-POM" section). Alternatively, the automatic sequence of calculations illustrated in Fig. 2 can be performed in real time. The illustrative graphical representation therein corresponds to the measured response of *PET/HS* filaments. As shown, the total OPD of the sample comprises three terms: (1) integer number of complete orders given by the number of minima counted in the plot from the melting temperature (where birefringence is nil) downwards; (2) if the part of the next incomplete order attains a maximum, this term values 275 nm; otherwise, it is nil; (3) the remaining section of the normalized light intensity curve is converted into the last portion of the total OPD following Eq. 1 for birefringent materials given by the Malus' law [5]. The total OPD will be determined by means of the formula and example presented in Fig. 2.

$$I = I_0 \sin^2\left(\frac{\pi}{\lambda}\mathrm{OPD}\right) \quad (1)$$

being I the cross-polarized transmitted light intensity, I_0 the initial cross-polarized transmitted light intensity, λ the light wavelength (550 nm for either green monochromatic light or average white light) and OPD the optical path difference (nm).

As for most optical techniques, the materials to be characterized must be sufficiently optically transparent (i.e., with limited light scattering from existing suspended particles/droplets). Thermally unstable systems, namely those undergoing unwanted chemical reactions during the thermal cycle, or those producing volatiles (which generate bubbles) are precluded (this includes foams). Furthermore, samples must have low surface roughness in order to minimize the contribution of superficial light scattering. Multiphasic systems with at least two components that are either crystalline and/or oriented can be studied, but the analysis is more complex and will not be pursued here.

The thermo-optical behavior of the PET filaments was analyzed in the 25–280 °C range, following a procedure similar to that adopted in the DSC experiments. The CSS 450 hot stage was thermally calibrated for a heating rate of 10 °C min^{-1} using an indium standard. The difference between the recorded melting temperature of indium and its standard known value ($T_m = 155.6$ °C) was input to the software and taken into account. In the case of aligned filaments, they were manually positioned on the hot stage at 45° relative to the crossed polarizers.

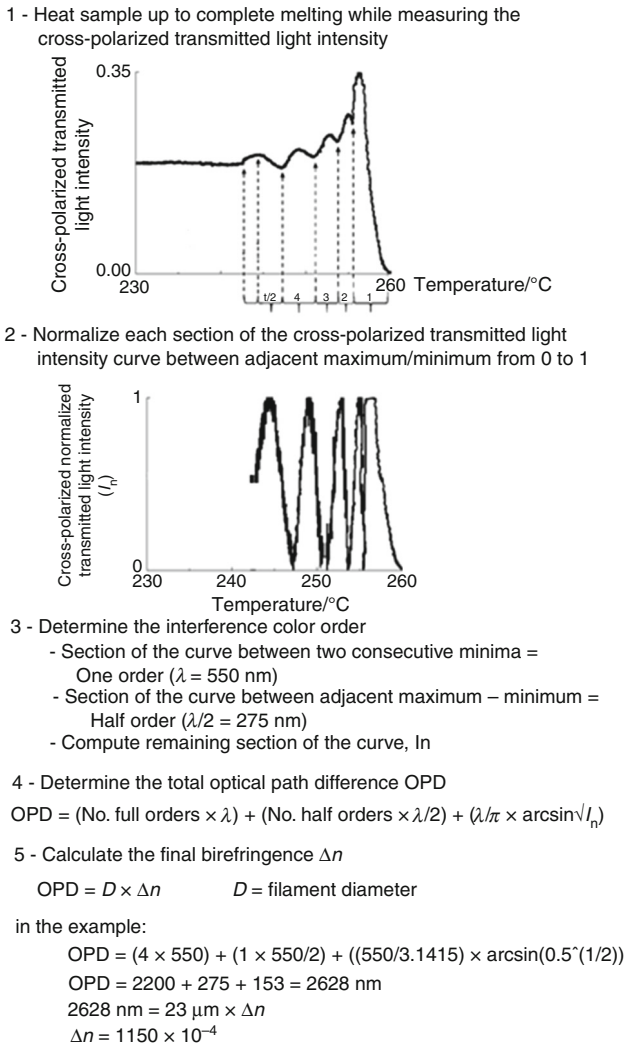

Fig. 2 Calculation sequence of the total optical path difference, OPD, from the minima/maxima pattern of the cross-polarized transmitted light intensity curve obtained during heating up the sample to its melting point (the example presented corresponds to the behavior of PET/HS)

Differential scanning calorimetry, DSC

A TA Instruments Differential Scanning Calorimeter, Q2000, was used to follow the evolution of heat flow with time during the thermal cycle imposed to each sample. The equipment was calibrated with an indium standard ($T_m = 155.6$ °C, $\Delta H = 6.8$ cal g^{-1}) at 10 °C min^{-1}. For the initial characterization and for comparison with q-

POM, filament samples weighting 6.5 ± 0.5 mg were finely chopped and placed inside an aluminum pan. After sealing, the lid was punctured and the assemblage was carefully flattened with a vise. This procedure was implemented in order to better guarantee adequate heat transfer between sample and furnace. After heating up to 280 °C at 10 °C min^{-1} under N_2 atmosphere (50 mL min^{-1}), the degree of crystallinity was computed from the first scan as Eq. 2:

$$\%\text{Crystallinity} = (\Delta H_m - \Delta H_c)/\Delta H_{100\%} \quad (2)$$

being ΔH_m the enthalpy of melting, ΔH_c the enthalpy of crystallization upon heating (known as cold crystallization) and $\Delta H_{100\%}$ the enthalpy of melting of a 100% PET crystalline sample, which was taken as 140 J g^{-1} [19]. All materials were tested at least twice.

Results and discussion

DSC versus q-POM

The thermo-optical behavior of the *PET/micro* multifilaments as analyzed by q-POM is shown in Fig. 3, together with the equivalent DSC curve (tested using identical thermal cycles). In the DSC curve (Fig. 3a), the change in the baseline at about 75 °C can be assigned to the glass transition of PET. An exothermic peak develops between approximately 85 and 145 °C due to the occurrence of cold crystallization, while melting takes place between 225 and 255 °C. The cross-polarized transmitted light intensity at the same heating rate and temperature range (Fig. 3b) shows several maxima and minima, indicating that the OPD passes through several optical orders. More importantly, these maxima and minima occur at the same temperature ranges associated with the thermal events in DSC. Upon heating from room temperature up to around 75 °C, the light intensity decreases due to relaxation of the stretched molecular structure, which is associated with the approximation of T_g. A sine-shaped curve develops from 85 to 255 °C. The first set of two maxima and two minima occurred between 85 and 145 °C, i.e., within the temperature interval where cold crystallization developed. Another set of two maxima and two minima are present between 225 and 255 °C, when melting takes place.

As discussed above, the cross-polarized transmitted light intensity curve does not directly yield the value of OPD, since the optical order of the filaments is unknown. One way to identify the retardation order involves recording simultaneously the cross-polarized transmitted light intensity and the colored digital images of the filaments as the sample is subjected to heating. This is shown in Fig. 4 for specific temperatures corresponding to relevant features of the cross-polarized transmitted light intensity versus temperature curve. In the figure, fibers may exhibit different colors, or different colors may be perceived for the same fiber. This is due to slight displacements of the fibers upon heating, thus leaving their deal position (aligned at 45° relative to the crossed polarizers). Using white light with average wavelength $\lambda = 550$ nm, Fig. 4 also identifies the maxima and minima of light intensity, which should occur for OPD values multiple of $\lambda/2 = 275$ nm. The OPD at room temperature (point 1 in Fig. 4) was measured as 408 nm with a Berek's compensator. From these values, and assuming constant filament diameter up to melting, birefringence values can be calculated, as depicted in Fig. 3c. As the temperature rises to 70 °C, birefringence remains essentially constant, declining to a minimum at a temperature slightly above the T_g of PET (this corresponds to point 3 in Fig. 4). As the temperature escalates, so does the birefringence, until reaching a maximum at 145 °C (point 9 in Fig. 4) due to cold crystallization, as detected by DSC. Beyond 145 °C, birefringence reduces progressively, though more pronouncedly between 225 and 255 °C, then vanishing due to melting of the filaments (points 12 to 15 in Fig. 4, corresponding to melting of the PET crystals).

In summary, as the temperature increases, the birefringence, as a bulk effect, reduces slightly from room temperature up to the T_g of PET ($\sim$75 °C); then, cold crystallization sets in, increasing the volumetric fraction of the crystalline phase and inducing an increase in the birefringence up to approximately 145 °C. Until 225 °C, no morphological changes are expected and so birefringence drops marginally, essentially due to the thermal expansion of the filaments. Between 225 and 255 °C, melting takes place, with swift vanishing of the crystalline volume fraction. As the filaments become optically isotropic, no optical retardation is produced, and thus, a sharp reduction in birefringence is observed.

Figure 3 includes also the variation in the turbidity of *PET/micro* filaments with temperature (Fig. 3d), in order to assess the sensitivity of this simple testing method to the thermophysical phenomena taking place. In this system, turbidity, i.e., the reduction in transmitted light intensity, is essentially produced by light scattering at the filament's surface. The increase in turbidity between approximately 45 and 70 °C (i.e., just below T_g of PET) is a complex summation of viscoelastic and optical effects. Upon approaching T_g, the amorphous chains both at the bulk and surface of the filaments increase mobility and relax. This phenomenon induces a reduction in the surface roughness with a corresponding increase in light scattering. As discussed above, in the 70–250 °C range no structural changes affect the surface of the filaments and so turbidity remains essentially constant (cold crystallization, developing in the 75–150 °C temperature range, is a bulk transformation).

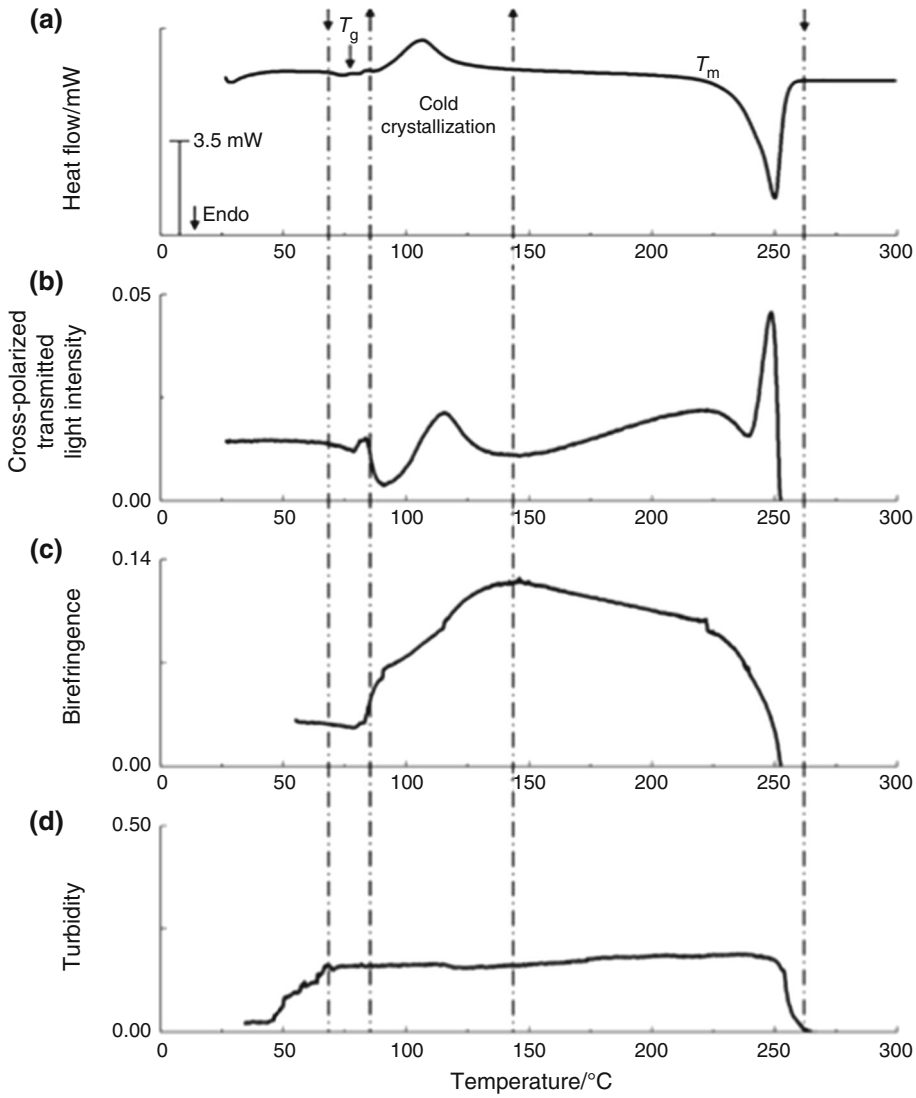

Fig. 3 Thermo-optical behavior of PET/micro multifilaments upon heating from room temperature up to melting, as measured by DSC and q-POM. **a** DSC curve; **b** cross-polarized transmitted light intensity; **c** birefringence (calculated from curve b); **d** turbidity

Turbidity reduces significantly with further increase in temperature, up to the PET melting point. This is due to shape distortion and amalgamation of the filaments, which reduce the interface area and thus light scattering. Amalgamation is probably more intense in the early stages of melting, due to the higher number of filaments, causing a sharp decrease in turbidity.

Sensitivity to variations in level of filament stretching and alignment

Filament stretching

Figure 5 shows information analogous to that of Fig. 3, but obtained for PET multifilaments with different levels of stretching (*PET/HS* and *PET/LS*). The DSC scans (Fig. 5a) show that the lesser stretched filament (*PET/LS*) has a lower degree of crystallinity and exhibits cold crystallization, which is revealed as a strong exothermal peak at a temperature range (from 75 up to 145 °C) above T_g of PET. Conversely, the highly stretched filaments are near to their maximum degree of crystallinity, presenting an almost imperceptible and broad peak at this same temperature range. In both cases, melting is shown as an endothermic peak occurring at the same temperature, thus indicating that the crystals thickness must be comparable. However, the higher enthalpy of *PET/HS* confirms its higher degree of crystallinity. These thermal effects are also detected in terms of cross-polarized transmitted light intensity (Fig. 5b). Cold crystallization, which is mostly present in *PET/LS*, is observed as a single pair of a maximum and a minimum above T_g, i.e., between 75 and 145 °C. In the case of *PET/HS*, changes in the trace within this temperature range are almost imperceptible, in agreement with the DSC scan. In the melting temperature range, the light intensity goes through a sequence of maxima/

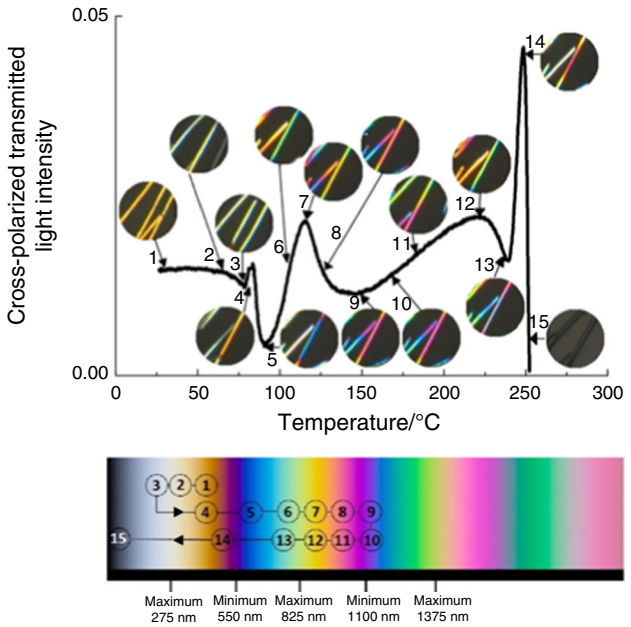

Fig. 4 Evolution with temperature of the cross-polarized transmitted light intensity of PET/micro filaments (same curve as in Fig. 3b). Digital images of the filament captured by the CCD camera at selected points (numbered from 1 to 15) show interference colors that are identifiable by the Michel–Levy's chart. Taking white light with average wavelength $\lambda = 550$ nm, the curve shows maxima and minima of light intensity that the chart identifies as having OPD values multiple of $\lambda/2 = 275$ nm

minima, showing interference fringes. A scan carried out at a slower heating rate of 1 °C min^{-1} yields a better resolution of the fringes for *PET/HS* (see inset of Fig. 5b), enabling the calculation of the total OPD according to the procedure presented in Fig. 2 (the example therein refers to the behavior of *PET/HS*), followed by the determination of the birefringence (Fig. 5c). The birefringence of *PET/HS* was estimated to be greater than 120×10^{-3} when using the Berek's compensator, a value of $115 \pm 5 \times 10^{-3}$ having been estimated with the procedure proposed here. This value remains constant up to the melting temperature range, when it reduces sharply. Contrariwise, *PET/LS* has very low birefringence at room temperature ($1.0 \pm 0.3 \times 10^{-3}$), which raises to $11.6 \pm 0.5 \times 10^{-3}$ with the contribution from cold crystallization and then remains constant up to the melting region, when it drops and levels off. Therefore, the differences in the levels of birefringence between the two filaments are significant and measurable by q-POM (see Table 2).

The results for turbidity are presented in Fig. 5d. Due to its high orientation and crystallinity, PET/HS exhibits high and mostly constant turbidity. Upon melting, a single-phase morphology is created, which drastically reduces the surface area and so the level of light scattering, thus inducing a decrease in turbidity to almost total transparency. As discussed above, *PET/LS* filaments develop cold crystallization, during which surface rearrangements increase turbidity. Both at lower and higher temperatures, turbidity is equivalent to that of PET/HS.

Table 2 summarizes the maximum changes in the thermo-optical properties of the three commercial filaments utilized in this study *(PET/micro, PET/LS and PET/HS)* upon heating from room temperature to complete PET filament melting. The changes in OPD and birefringence were acquired by q-POM, while crystallinity data were obtained from DSC experiments performed under similar conditions. Equation 2 was used to calculate the initial crystallinity, all maxima being computed after cold crystallization.

Filament alignment

It is also interesting to check whether filament alignment (i.e., geometrical positioning) influences the values of birefringence calculated in real time. In order to investigate this, composite films of LLDPE/*PET/micro* filaments aligned in a single direction and randomly distributed were analyzed. It is anticipated that the corresponding cross-polarized transmitted light intensity curves will be distinct, as the angle of the filaments relative to the cross-polarizers will be different and so will be their contribution. However, the birefringence value should be the same, since it is a bulk (physical) characteristic of the sample. The results for composite films containing aligned and randomly distributed filaments are presented in Fig. 6. The former were positioned in the hot stage with all filaments set at 45° to the cross-polarizers, to maximize the optical effect. Composite films with randomly aligned filaments were placed without any particular rule. The response of the pristine LLDPE film is provided in Fig. 7, to facilitate the interpretation of the thermal and optical behavior of the composite. Although the DSC trace shows a melting peak at 115 °C, the cross-polarized transmitted light intensity detects a much broader melting range, with progressive reduction in crystallinity, starting from room temperature onwards.

As expected, the DSC curve of the composite film (Fig. 6a) displays the individual thermal events of each of its components, such as melting peaks. In contrast to Fig. 3a, melting of the PET filaments produces a double peak. This behavior has been observed previously on both drawn and undrawn PET samples [13, 20, 21] and attributed either to a melting and recrystallization process [20] or to morphological changes induced by drawing [21]. As explained in "Materials" section, pans containing samples to be characterized by DSC were flattened under pressure in order to better guarantee adequate heat transfer between sample and DSC furnace. Nonetheless, samples not

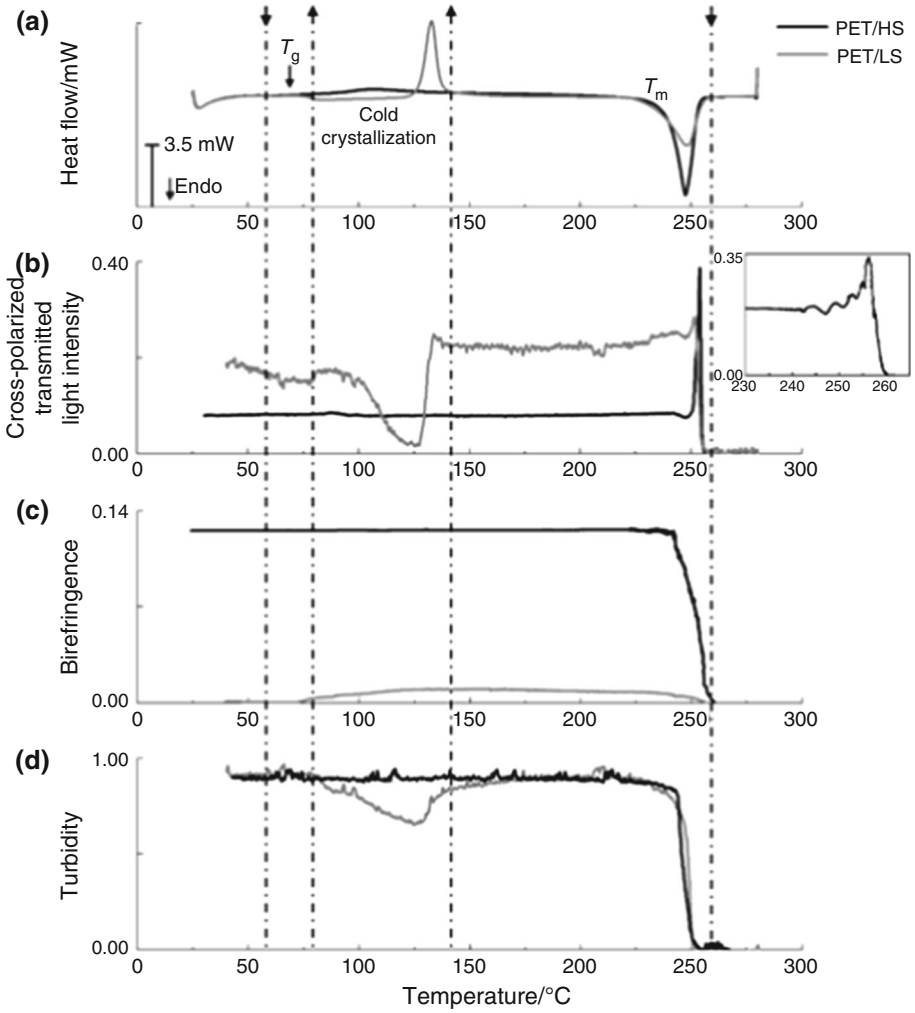

Fig. 5 Thermo-optical behavior of PET/HS and PET/LS multifilaments upon heating from room temperature up to melting, as measured by DSC and q-POM. **a** DSC curve; **b** cross-polarized transmitted light intensity (inset is a magnification of the melting peak of PET/HS measured at 1 °C min^{-1}); **c** birefringence (calculated from curve b); **d** turbidity

Table 2 Increase in the original OPD, birefringence and crystallinity of PET filaments upon heating

Type of PET multifilament	OPD/nm		Birefringence/$\times 10^{-3}$		Crystallinity[d]/%	
	Initial[a]	Maximum[b,c]	Initial	Maximum[c]	Initial	Maximum[c]
PET/micro	408 ± 15	1100 ± 50	47 ± 2	122 ± 5	24 ± 2	38 ± 2
PET/LS	52 ± 7	630 ± 15	1.0 ± 0.3	11.6 ± 0.5	10 ± 2	30 ± 2
PET/HS	> 2750	2628 ± 50	> 120	115 ± 5	35 ± 2	40 ± 2

[a] Measured with a Berek's compensator

[b] Measured by the procedure presented here

[c] After cold crystallization

[d] Measured from DSC

subjected to this procedure also exhibited the double melting peak. This seems to indicate that the presence of a second medium (polyethylene, in the case of the composite films) and/or of entrapped air in samples prepared in the usual way interferes negatively with the heat flow and so with the measurement.

The above artifact is exclusive to the DSC trace and does not affect the cross-polarized transmitted light intensity measurements, which are presented in Fig. 6b. The shape of the two curves is comparable, particularly close to the PET melting range, but the signal intensity is higher for the composite with aligned filaments. Indeed, the cross-polarized transmitted light intensity reveals the level of

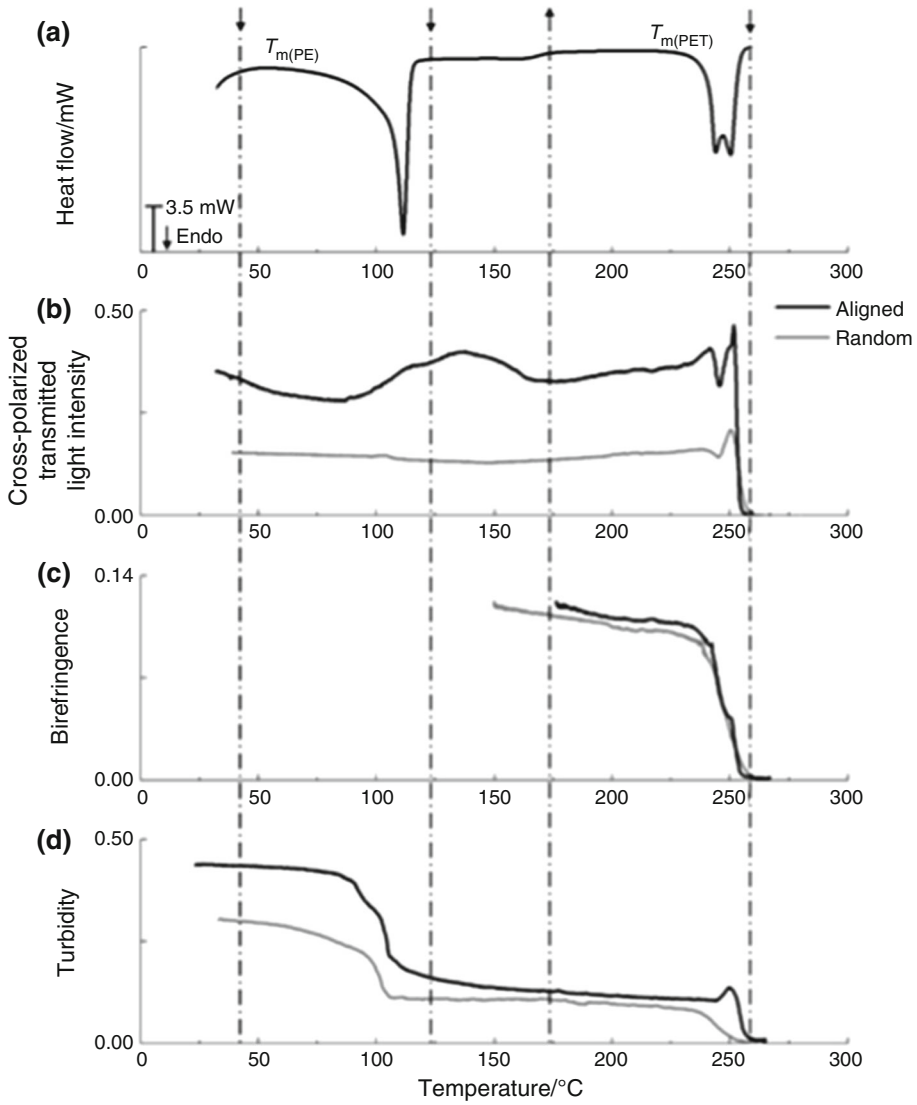

Fig. 6 Thermo-optical behavior of LLDPE/PET/micro composite films containing aligned and randomly distributed filaments upon heating from room temperature up to melting of PET, as measured by DSC and q-POM. **a** DSC curve; **b** cross-polarized transmitted light intensity; **c** birefringence (calculated from curve b); **d** turbidity

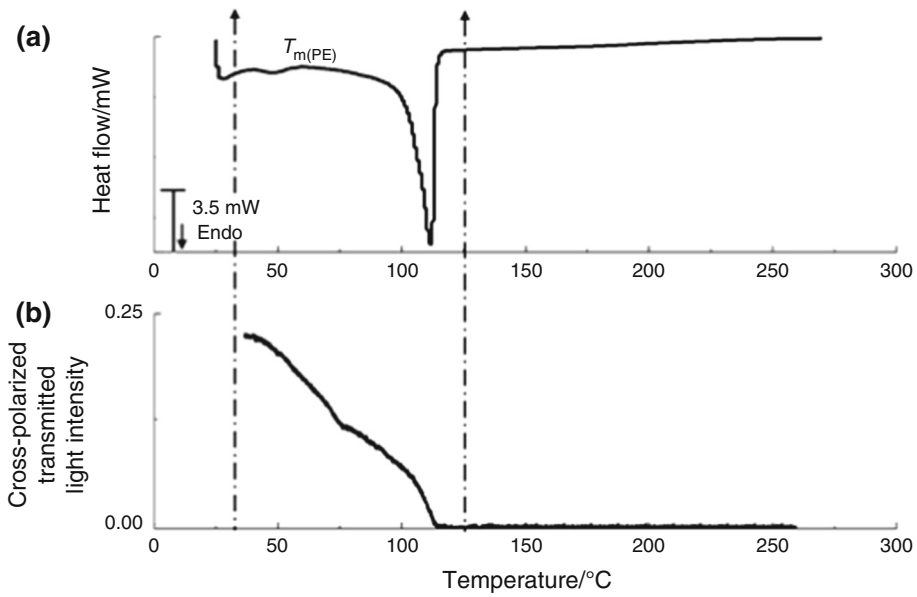

Fig. 7 Thermo-optical behavior of LLDPE, as measured by DSC and q-POM. **a** DSC trace and **b** cross-polarized transmitted light intensity by q-POM

crystalline orientation, but depends on its alignment with the cross-polarizers. Nonetheless, the calculated birefringence of the two samples is equivalent (Fig. 6c) if using the method proposed, and based on counting the number of maxima/minima.

As before, turbidity was measured simultaneously, in real time. In the case of composites, turbidity depends on the light scattering produced by interphases with sufficiently different refractive indices. Thus, geometric factors such as number of particles and corresponding size and shape are dominant. In the specific case of the PE/PET filament system, two interfaces are present, between crystalline and amorphous phases in the polyethylene matrix and between the PE matrix and the PET filaments. At temperatures below T_m of PE, its crystalline phase scatters light, generating a milky material with significant turbidity. Upon melting of PE, the contribution to turbidity will arise exclusively from the interface between the molten PE matrix and the PET filaments. If the filaments are aligned in a single direction, they all interact with the traversing light, and so the amount of interface is fully quantified. If they are randomly distributed, portions of filaments will become cross-piled, i.e., portions of filaments that are covered by others will not scatter light, hence reducing the global turbidity.

Conclusions

An experimental setup and associated calculation method were presented with the aim of analyzing in real time the thermal events usually characterized by DSC, as well as quantifying birefringence and turbidity. The technique was applied to samples of commercial PET multifilaments with different initial crystallinity and stretching levels.

Upon subjecting the samples to identical heating runs, it was demonstrated that DSC and transmitted light intensity detected the same thermal transitions, which extended through identical temperature ranges. If measurement of the cross-polarized transmitted light intensity was accompanied by simultaneous recording of filament images with a color CCD camera, the optical path difference could be determined from color interpretation using Michel–Levy's chart. In turn, this enabled the determination of birefringence. An alternative automatic real-time calculation procedure based on the analysis of the minima/maxima pattern of normalized cross-polarized transmitted light intensity curves was proposed, yielding matching data. Birefringence was shown to be sensitive to different filament stretching levels, but remained unaffected by geometrical parameters such as geometrical filament alignment. Turbidity—a straightforward measurement—displayed similar sensitivity, but changed with filament alignment.

The results demonstrated the feasibility of obtaining quantitative data on crystallinity and orientation levels using optical techniques and procedures that can be automated. Thus, the next step of this work will consist in developing an inexpensive device to be used in the production floor, or directly in-line, for practical quality assessment/control.

Acknowledgements The authors would like to acknowledge UNIFI, ECOFABRIL and DOW, Brazil, for donating materials, as well as Coordenação de Aperfeiçoamento de Pessoal de Nível Superior (CAPES) for scholarship to L. A. Bicalho, grant BJT 019/2012 to J. M. J. Silva, grant PVE 30484/2013-01 to J. A. Covas and Conselho Nacional de Desenvolvimento Científico e Tecnológico (CNPq) for a PQ scholarship 311790/2013-5 to S. V. Canevarolo. The assistance of the technicians from DEMa is also gratefully acknowledged.

References

1. Sondergaard K, Lyngaae-Jorgensen J. Rheo-physics of multiphase polymer systems. Lancaster, PA: Technomic Publishing Co., Inc; 1995.
2. Young V. Instrumental Methods of Analysis, Seventh Edition (Dean, John A.; Merritt, Lynne L., Jr.; Settle, Frank A., Jr.; Willard, Hobart H.). J Chem Educ. 1989;66(1):A46. doi:10.1021/ed066pA46.2.
3. Schindler A, Doedt M, Gezgin Ş, Menzel J, Schmölzer S. Identification of polymers by means of DSC, TG, STA and computer-assisted database search. J Therm Anal Calorim. 2017;129(2):833–42. doi:10.1007/s10973-017-6208-5.
4. Mathot VBF. Crystallization of polymers. J Therm Anal Calorim. 2010;102(2):403–12. doi:10.1007/s10973-010-0947-x.
5. Meeten GH. Optical properties of polymers. Amsterdam: Springer; 1986.
6. Magill JH. A new method for following rapid rates of crystallization I. Poly(hexamethylene adipamide). Polymer. 1961;2:221–33. doi:10.1016/0032-3861(61)90025-8.
7. Magill JH. A new technique for following rapid rates of crystallization II isotactic polypropylene. Polymer. 1962;3:35–42. doi:10.1016/0032-3861(62)90064-2.
8. Ding Z, Spruiell JE. An experimental method for studying nonisothermal crystallization of polymers at very high cooling rates. J Polym Sci Part B Polym Phys. 1996;34(16):2783–804. doi:10.1002/(SICI)1099-0488(19961130)34:16<2783:AID-POLB12>3.0.CO;2-6.
9. Supaphol P, Spruiell JE. Nonisothermal bulk crystallization studies of high density polyethylene using light depolarizing microscopy. J Polym Sci Part B Polym Phys. 1998;36(4):681–92. doi:10.1002/(SICI)1099-0488(199803)36:4<681:AID-POLB14>3.0.CO;2-B.
10. Supaphol P, Spruiell JE. Nonisothermal bulk crystallization of high-density polyethylene via a modified depolarized light microscopy technique: further analysis. J Appl Polym Sci. 2002;86(4):1009–22. doi:10.1002/app.11121.
11. da Cunha Santos AM, Cáceres CA, Calixto LS, Zborowski L, Canevarolo SV. In-line optical techniques to characterize the polymer extrusion. Polym Eng Sci. 2014;54(2):386–95. doi:10.1002/pen.23569.
12. Mould ST, Barbas JM, Machado AV, Nóbrega JM, Covas JA. Monitoring the production of polymer nanocomposites by melt compounding with on-line rheometry. Int Polym Proc. 2012;27(5):527–34. doi:10.3139/217.2597.

13. Zborowski L, Canevarolo SV. In-line turbidity monitoring of the second phase droplets deformation during extrusion. Polym Eng Sci. 2013;53(11):2422–8. doi:10.1002/pen.23490.
14. De Clerck K, Rahier H, Van Mele B, Kiekens P. Thermal properties relevant to the processing of PET fibers. J Appl Polym Sci. 2003;89(14):3840–9. doi:10.1002/app.12543.
15. Halliday D, Resnick R, Walker J. Fundamentals of Physics. New York: Wiley; 2010.
16. Hecht E. Optics, 3 ed. Reading, MA: Addison-Wesley; 1998.
17. Berl JH. Master Thesis, Universidade Federal de São Carlos. 2015.
18. Berl JH, da Cunha Santos AM, Lucas AA, Canevarolo SV, editors. Quantitative characterization of polymer crystallization via instrumented polarized light optical microscopy. Regional Meeting da Polymer Processing Society PPS-Tel Aviv; 2014; Tel Aviv.
19. van Krevelen DW, te Nijenhuis K. Properties of polymers: their correlation with chemical structure; their numerical estimation and prediction from additive group contributions, 4th ed. Amsterdam: Elsevier; 2009.
20. Fakirov S, Fischer EW, Hoffmann R, Schmidt GF. Structure and properties of poly(ethylene terephthalate) crystallized by annealing in the highly oriented state: 2. Melting behaviour and the mosaic block structure of the crystalline layers. Polymer. 1977;18(11):1121–9. doi:10.1016/0032-3861(77)90105-7.
21. Elenga R, Seguela R, Rietsch F. Thermal and mechanical behaviour of crystalline poly(ethylene terephthalate): effects of high temperature annealing and tensile drawing. Polymer. 1991;32(11):1975–82. doi:10.1016/0032-3861(91)90161-B.